

UDC 549.07/753.1:53.091

Mechanochemical Synthesis of Hydroxyapatite with SiO_4^{4-} Substitutions

M. V. CHAIKINA¹, N. V. BULINA¹, I. YU. PROSANOV¹, A. V. ISHCHEKNO², O. V. MEDVEDKO³ and A. M. ARONOV³¹*Institute of Solid State Chemistry and Mechanochemistry, Siberian Branch of the Russian Academy of Sciences, Ul. Kutateladze 18, Novosibirsk 630128 (Russia)**E-mail: chaikinam@solid.nsc.ru*²*Boreskov Institute of Catalysis, Siberian Branch of the Russian Academy of Sciences, Pr. Akademika Lavrentyeva 5, Novosibirsk 630090 (Russia)*³*NEVZ-SOYUZ JSC, Krasny Pr., 220, Novosibirsk 630049 (Russia)*

(Received November 10; revised February 10, 2012)

Abstract

Using the mechanochemical method during 30 min in the planetary mill, we synthesized the samples of hydroxyapatite (HAP) modified with silicate ions in the amount of 0.1, 0.2, 0.4 and 0.8 molar fractions of the ion SiO_4^{4-} in HAP at the given molar ratio $\text{Ca}/(\text{P} + \text{Si}) = 1.67$. As a result of activation in the air medium, hydroxyapatite with the average crystallite size of ~20 nm was formed. The mechanochemically synthesized samples contain carbonate ion substituting the phosphate ion, with the formation of carbonatehydroxyapatite of B type; its amount decreases with an increase in the amount of silicate introduced. Modification of hydroxyapatite with silicate ions is a competing reaction for phosphate substitution with carbonate. Depending on the ratio of silicate to carbonate amounts in hydroxyapatite structure, the mechanism of substitution changes. In the case of predominance of the carbonate ion in apatite, the composition corresponds to the general formula $\text{Ca}_{10 - (x - y)/2}(\text{PO}_4)_{6 - (y + x)}(\text{SiO}_4)_y(\text{CO}_3)_x(\text{OH})_2$ ($x > y$). In the case of the equal number of substituents ($x = y$) silicate-substituted hydroxyapatite has the stoichiometric composition with the general formula $\text{Ca}_{10}(\text{PO}_4)_{6 - (y + x)}(\text{SiO}_4)_y(\text{CO}_3)_x(\text{OH})_2$. In the case of predominance of silicate ion ($x < y$), charge compensation occurs due to the formation of vacancies in the positions of $(\text{OH})^-$ groups: $\text{Ca}_{10}(\text{PO}_4)_{6 - (y + x)}(\text{SiO}_4)_y(\text{CO}_3)_x(\text{OH})_{2 - y}$. After annealing the samples, the silicate group occupies the positions of phosphate ion in hydroxyapatite structure with the formation of vacancies in the positions of $(\text{OH})^-$ group; the composition is described by the general formula $\text{Ca}_{10}(\text{PO}_4)_{6 - x}(\text{SiO}_4)_x(\text{OH})_{2 - x}$.

Key words: mechanochemical synthesis, silicate-substituted hydroxyapatite

INTRODUCTION

Hydroxyapatite (HAP) $\text{Ca}_{10}(\text{PO}_4)_6(\text{OH})_2$ is the major mineral component of bone and tooth tissues of humans and animals. Natural HAP does not correspond to this idealized formula and always contains cation and anion substitutions in its structure (from several hundredth parts to several mass per cent) playing essential biological role. The compounds with apatite structure possess dynamic structure allowing a broad range of substitutions. During the recent

decades, the varieties of HAP with substitutions are investigated to assess the possibility of using them as materials for medical purposes: as coatings for implants, biocompatible ceramics, medicinal and cosmetic means [1–3]. One of the substituents in the anion sublattice of HAP is SiO_4^{4-} ion. Many studies dealt with the effect of the partial substitution of phosphate for silicate group in HAP structure on its physicochemical and biological properties [4–11]. Investigations carried out *in vitro* and *in vivo*, with cell cultures and with various animals

showed that ceramics made of silicate-substituted HAP (Si-HAP) promotes more rapid implantation in comparison with HAP samples containing no silicate ion [12–14]. According to the literature data, this is connected with the surface properties of the samples [14–17].

The authors of [15, 16] relate the high surface activity of Si-HAP with the formation of silanol groups $-\text{SiOH}$ on the surface of the materials. These groups take an active part in interface mineralization. According to the data reported in [15], due to the differences in the size of tetrahedral anions (the distances $\text{Si}-\text{O} = 0.166$ nm, $\text{P}-\text{O} = 0.155$ nm) the substitution of phosphate ion for the silicate one is accompanied by the appearance of microstrain in apatite structure. As a result, silicate ions get segregated on the surface of particles. The authors of [16] also explain the high values of Z potential at the initial moment of hydrolysis of HAP samples modified with silicon by the segregation of silicate ions on sample surface. Investigation of the surface of Si-HAP coatings deposited by means of high-frequency magnetron sputtering on metal substrates showed that their electrostatic potential increases in comparison with the samples without substitution [16]. As a consequence of the roughness of coatings, complication of their relief was accompanied by strengthening of the electret potential. The cell cultures of bone marrow deposited on these coatings in model biological electrolyte modulated the amplitude and leveled scattering of the surface electrostatic potential of the coatings [16].

The most thorough investigation of comparative electrostatic and adhesion properties of the surface of Si-HAP samples with Si mass fraction 0.8 % and HAP of stoichiometric composition was carried out by the authors of [17]. The electrochemical characteristics of the surface of polycrystalline SiO_4^{4-} -substituted HAP samples and HAP without substitution were obtained with the help of high-resolution force spectroscopy using the method of self-organized monolayers of COO terminal alkane thiols. The authors of [17] established that the samples of Si-substituted HAP are characterized by higher values of Van der Waals interactions in comparison with unsubstituted sample. This is evidenced by the obtained values of Hamaker con-

stants which are two times larger for Si-HAP than for stoichiometric HAP. Using the theory of Deryagin–Landau–Ferway–Overbeck and non-linear Poisson–Boltzmann model, the authors calculated the values of surface charges for the forces of the electrostatic double layer. These values turned out to be negative, two times larger for Si-HAP than for pure HAP. The adhesion of the surface layer of Si-HAP particles was also higher than the adhesion of stoichiometric HAP [17]. The obtained data explain the positive effect of the partial substitution of phosphate by silicate ion in the model experiments on cell propagation *in vitro* and active bone formation and substitution of bone tissues in the studies of samples *in vivo* [6, 13–16].

Several ten works deal with the methods of the synthesis of HAP with the partial substitution of phosphate ion by SiO_4^{4-} ; these works were generalized in review articles and monographs [1–15]. HAP modified with silicate ion is obtained using different methods and from different initial components. In the majority of works, the synthesis of modified HAP is carried out by precipitation from the solutions of phosphate salts or phosphoric acid, calcium hydroxide suspension and soluble silicon compounds [8–15]. Synthesis from solutions is a labour-intensive and long-term process resulting in the formation of non-monophase products. The synthesis through the sol-gel procedure and hydrothermal method are not less complicated [18–23]. In some works, corals and even cuttlefish shells were used as the basis of bioceramics for the synthesis of apatite and composite [13, 25].

The mechanochemical method of the synthesis of apatite species is promising [26–29]. Many works on the synthesis of HAP and its species with various substituents appeared during the past decade [30–37]. However, in the majority of works the authors fail to obtain apatite in the form of well arranged crystalline product directly in the mill. In [33, 35, 36], broad reflections were revealed using the X-ray phase method; these reflections provide evidence of the formation of apatite only after annealing or mechanical activation for at least 5–6 h. In some works, the reaction is carried out in the liquid phase [23, 30], or $\text{Ca}(\text{OH})_2$ and P_2O_5 are used as the initial materials, which

is also close to the liquid-phase synthesis because of hydration of phosphorus oxide. During the liquid-phase synthesis, the action is reduced to component mixing, so these versions cannot be related to direct mechanochemical methods. The authors of [23] subjected the reaction mixture after mechanical activation to hydrothermal treatment.

Works on the mechanochemical synthesis of HAP modified by silicate ions are unavailable in literature at present, except for the work [23] where the synthesis was carried out using the wet procedure.

The search for the optimal compositions of modified HAP species as coatings for implants made of titanium, its alloys, zirconium and aluminium oxide ceramics, promoting osteosynthesis on implants is important problem. According to the data of the authors of [5] who studied the effect of the concentration of silicon substituting phosphate in HAP during implantation in white rabbits of New Zealand, the optimal concentration is 0.8 % Si. However, this question remains disputable, and the concentrations of phosphate substitution by silicate are studied within a broad range from one tenth to several molecules per cell [10].

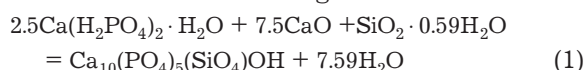
In the present work we studied the mechanochemical synthesis of HAP modified with different amounts of SiO_4^{4-} ions with the general formula of the given composition: $\text{Ca}_{10}(\text{PO}_4)_{6-x}(\text{SiO}_4)_x(\text{OH})_{2-x}$, where $x = 0.1, 0.2, 0.4, 0.8$, and examined the state of its structure after annealing of the sample. These prod-

ucts may be used in future as the material to coat implants [38].

EXPERIMENTAL

We chose the initial components for the synthesis of HAP with the partial substitution of phosphate by SiO_4^{4-} ion to be $\text{Ca}(\text{H}_2\text{PO}_4)_2 \cdot \text{H}_2\text{O}$, CaHPO_4 , CaO and amorphous $\text{SiO}_2 \cdot n\text{H}_2\text{O}$ with specific surface 400–420 m^2/g , $n = 0.59\text{--}0.71$.

To study the process of the interaction of the components of mechanochemical synthesis, we prepared the sample using $\text{Ca}(\text{H}_2\text{PO}_4)_2 \cdot \text{H}_2\text{O}$ as the initial phosphate. The interaction between the components in this case was carried out according to reaction



This process was accompanied by substantial aggregation, so CaHPO_4 was used as the initial phosphate for the synthesis of other samples. The reaction of mechanochemical synthesis and the codes of resulting samples are presented in Table 1.

Mechanochemical synthesis of the samples was carried out using the planetary mill AGO-2 in water-cooled steel cylinders 150 mL in volume, with steel balls with the mass of 200 g, at the frequency of cylinder rotation 1200 min^{-1} for 30 min. The ratio of the weighted portion of reaction mixture to ball mass was 1 : 10.

To avoid metal wear, the working zone of the mill was lined with the reaction mixture of the components of the sample to be syn-

TABLE 1
Mechanochemical synthesis of Si-HAP samples

Reaction of mechanochemical synthesis	Given product composition	Sample codes	
		before thermal treatment	after thermal treatment
$6\text{CaHPO}_4 + 4\text{CaO} = \text{Ca}_{10}(\text{PO}_4)_6(\text{OH})_2$	$\text{Ca}_{10}(\text{PO}_4)_6(\text{OH})_2$	HAP-0	HAP-0T
$5.9 \text{CaHPO}_4 + 4.1\text{CaO} + 0.1\text{SiO}_2 \cdot 0.71\text{H}_2\text{O} \\ = \text{Ca}_{10}(\text{PO}_4)_{5.9}(\text{SiO}_4)_{0.1}(\text{OH})_{1.9} + 2.071\text{H}_2\text{O}$	$\text{Ca}_{10}(\text{PO}_4)_{5.9}(\text{SiO}_4)_{0.1}(\text{OH})_{1.9}$	HAP-01	HAP-01T
$5.8\text{CaHPO}_4 + 4.2\text{CaO} + 0.2 \text{SiO}_2 \cdot 0.71\text{H}_2\text{O} \\ = \text{Ca}_{10}(\text{PO}_4)_{5.8}(\text{SiO}_4)_{0.2}(\text{OH})_{1.8} + 2.142\text{H}_2\text{O}$	$\text{Ca}_{10}(\text{PO}_4)_{5.8}(\text{SiO}_4)_{0.2}(\text{OH})_{1.8}$	HAP-2	HAP-2T
$5.6\text{CaHPO}_4 + 4.4\text{CaO} + 0.4\text{SiO}_2 \cdot 0.71\text{H}_2\text{O} \\ = \text{Ca}_{10}(\text{PO}_4)_{5.6}(\text{SiO}_4)_{0.4}(\text{OH})_{1.6} + 2.284\text{H}_2\text{O}$	$\text{Ca}_{10}(\text{PO}_4)_{5.6}(\text{SiO}_4)_{0.4}(\text{OH})_{1.6}$	HAP-04	HAP-04T
$5.2\text{CaHPO}_4 + 4.8\text{CaO} + 0.8\text{SiO}_2 \cdot 0.71\text{H}_2\text{O} \\ = \text{Ca}_{10}(\text{PO}_4)_{5.2}(\text{SiO}_4)_{0.8}(\text{OH})_{1.2} + 2.568\text{H}_2\text{O}$	$\text{Ca}_{10}(\text{PO}_4)_{5.2}(\text{SiO}_4)_{0.8}(\text{OH})_{1.2}$	HAP-08	HAP-08T

thesized. As a result, the surface of balls and cylinder walls was coated with this mixture. The mixture was removed after 1 min from the start of activation, and then the synthesis of HAP was carried out. According to the data of analysis, iron content in mechanochemically synthesized HAP samples did not exceed 0.03–0.05 mass %.

The content of carbonate ion appearing in the structure of HAP samples due to absorption of CO₂ from the air was determined by means of gas manometer method (by dissolving the weighted portion in 10 mL of HCl with the density of 1.08 g/cm³) [39].

Annealing of the samples was carried out in a high-temperature electric box furnace PVK-1.4-8 at 1000 °C for 5 h.

The stages of mechanochemical synthesis and the final products were studied by means of high-resolution transmission electron microscopy (HRTEM) and energy dispersive X-ray microanalysis (EDX) with the JEOL transmission electron microscope. The final product was studied by means of IR spectroscopy with an Infracum-801 spectrometer and by means of X-ray diffraction using D8 Advance powder diffractometer. X-ray diffraction patterns were recorded in Bragg-Brentano geometry with CuK_α radiation, nickel K_β filter and superfast position-sensitive one-dimensional Lynx-Eye detector (angle of bite 3°). Tablets of samples were pressed with KBr for IR spectroscopy.

X-ray phase analysis of the synthesized compounds was carried out using EVA programme [40] and the database of powder diffraction patterns ICDD [41]. The refinement of the unit cell parameters of substituted HAP and quantitative analysis according to Rietveld procedure were carried out with the help of TOPAS programme [42]. Initial structural parameters of HAP and CaO were taken from the structural database (supplement to TOPAS programme); the data on the parameters of Ca(OH)₂ and CaHPO₄ were taken from the crystallographic database ICSD [43]. The average size of crystallites (coherent length) was calculated from the integral broadening of the peaks according to Sherrer's procedure. It was assumed that the contribution from microstrain into peak broadening was equal to zero. In the description of line profile, the instrumental

function was determined by means of fundamental parameters [44].

RESULTS AND DISCUSSION

It was shown in [32] that the interaction between components during mechanical activation can proceed through the amorphous state and/or on the surface of phases according to the topotaxial mechanism, depending on the physicochemical properties of initial substances and the relations between the structures of initial phosphate and synthesized HAP with hexagonal group.

The stages of the interaction between the components during the mechanical synthesis of Si-HAP were visualized with the help of HRTEM; the changes of the composition of the mixture were followed by means of energy dispersive X-ray analysis (Figs. 1, 2). Similarly to activation in the mill [27], under the electron beam of the microscope the initial phosphate Ca(H₂PO₄)₂ · H₂O interacts with CaO since the first seconds, with the formation of CaHPO₄ (see Fig. 1, a). This is confirmed by the EDX data: the ratio Ca/P = 1 in the inner part of the nanoparticle marked with circle 2, which corresponds to monetite CaHPO₄ composition, while the outer shell of the nanoparticle is composed of initial Ca(H₂PO₄)₂ · H₂O (circle 1, where Ca/P = 0.5, see Fig. 1, a). In the part of the sample adjacent to the nanoparticle from the outer side (circle 3) the content of Ca, P and Si is approximately the same (see Fig. 1, a). Changes of the state of phosphate and silicon oxide under the effect of electron beam of the microscope is shown in Fig. 1, b. Silicon oxide (circle 3) is gradually "absorbed" by amorphous phosphate, and at the stage of the last frame (see Fig. 1, b), according to EDX data, the reaction mixture is composed of nanoparticles of different compositions. In the region of circle 1, the particle of unreacted SiO₂ is present; in circle 2, there is a spherical particle of amorphous substance which corresponds in its composition to calcium-deficient apatite Ca₉(HPO₄)_{6-x}(SiO₄)_x(OH)_{2-x} residual SiO₂ (not "absorbed" by phosphate) is in circle 3; circle 4 marks the product CaHPO₄. The interaction between the components can

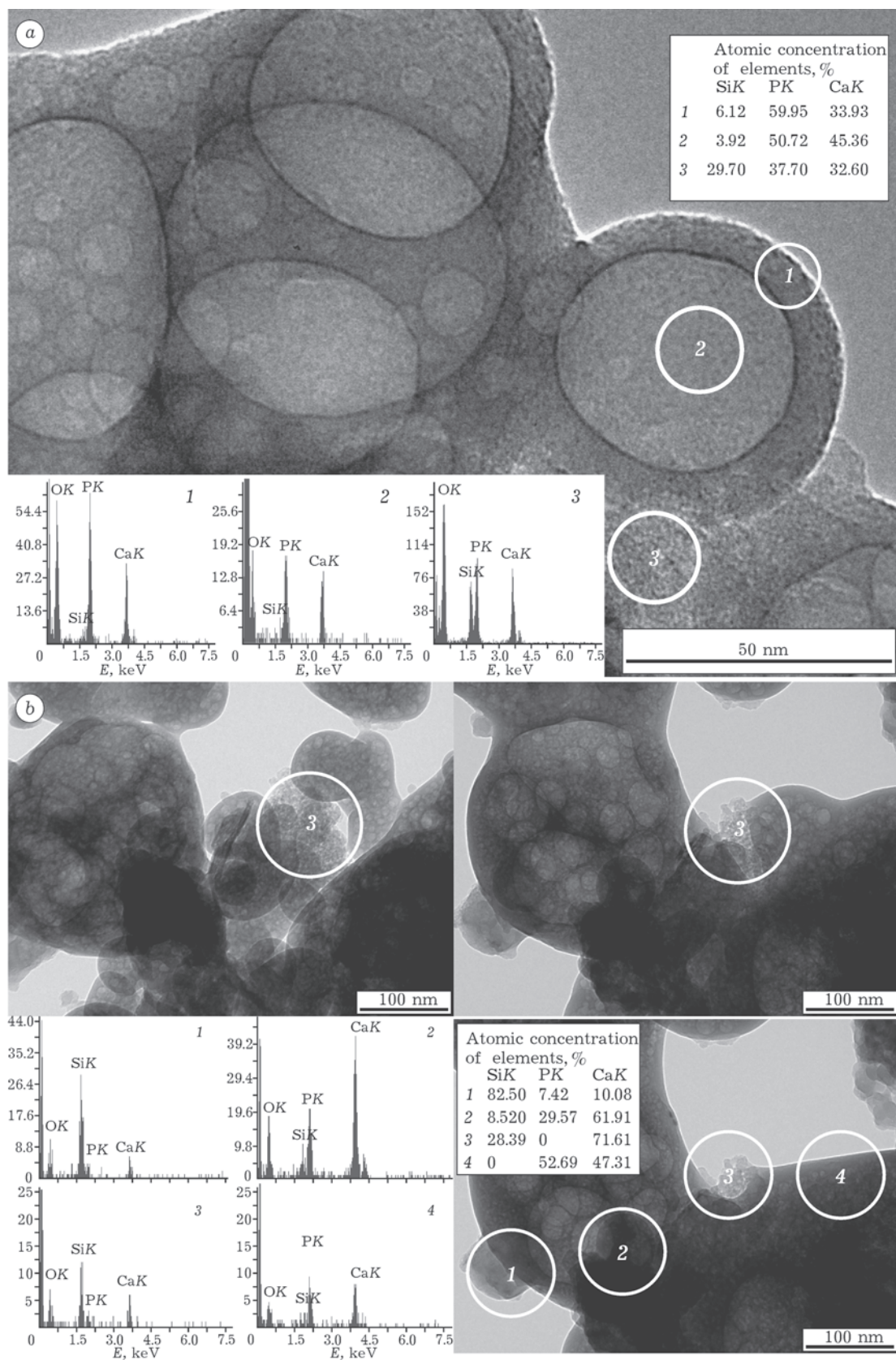
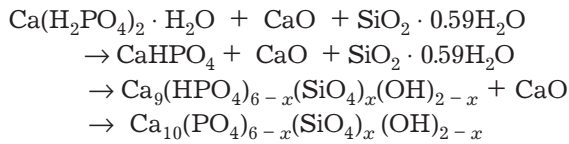


Fig. 1. EM images and EDX data on the state of reaction mixture described in equation (1), after mechanical activation for 30 s (a), 10 min (b).

be represented as a sequence of neutralization reactions characteristic of the soft mechanochemical synthesis [26]:



After mechanical activation of the mixture of reagents in AGO-2 mill for 30 min, the resulting samples are the aggregates of crystalline particles (Fig. 2, *a*) with extended lattice (see Fig. 2, *b*). According to EDX data, mechanochemically synthesized samples contain a definite amount of silicon. However, this amount can differ from the values presented in Table 1 because silicon is partly in the amorphous state. This is also confirmed by the results of HRTEM (see Fig. 2, *b*): along with nanocrystalline HAP particles, the amorphous phase is observed in the upper left corner of the image.

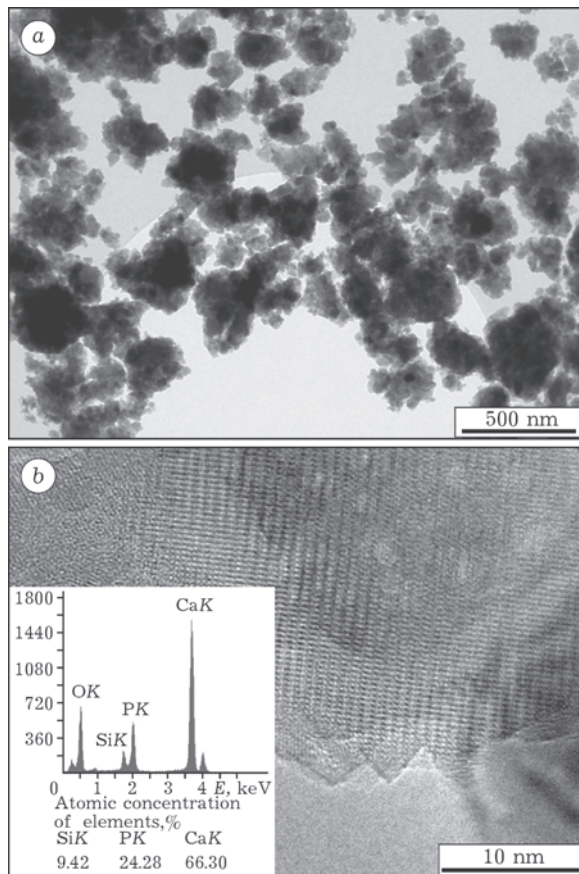


Fig. 2. EM images of HAP-88 sample before annealing: *a* – general view, *b* – HRTEM and EDX.

After annealing, the samples appear as dense aggregates of sintered particles (Fig. 3, *a*). Small CaO crystals are observed in the upper left corner. These crystals could be formed as a result of carbonate apatite decomposition. According to the data of HRTEM and EDX, after annealing the samples have extended lattice and the composition corresponding to the given one: $\text{Ca}_{10}(\text{PO}_4)_{5.2}(\text{SiO}_4)_{0.8}(\text{OH})_{1.2}$ (see Fig. 3, *b*).

The IR spectra of mechanochemically synthesized Si-HAP samples before annealing are shown in Fig. 4, *a*, *b*. The IR spectra are characterized by the following absorption bands corresponding to the vibrations of P–O bonds in apatite structure: bending ν_4 (O–P–O) within the wavenumber range $570\text{--}600\text{ cm}^{-1}$ and stretching ν_3 within the range $1000\text{--}1050\text{ cm}^{-1}$ see Fig. 4, *a*). A weak band at 3575 cm^{-1} is due to the vibrations of the bonds of OH group localized in the channels along the 6_3 axis of

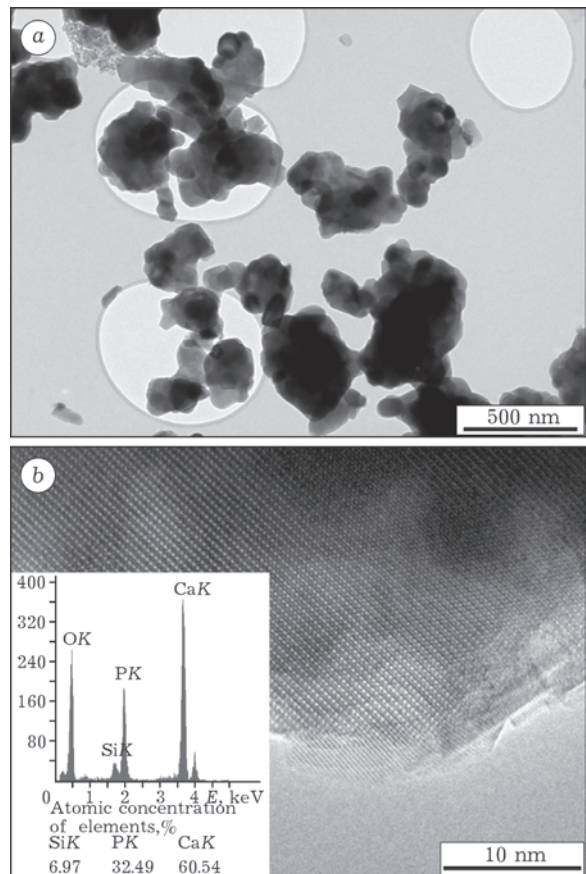


Fig. 3. EM images of HAP-88T after annealing: *a* – general view, *b* – HRTEM and EDX.

HAP structure [2]. After the synthesis of HAP in air, CO_3^{2-} ion and a small amount of adsorbed water are always detected its structure by means of IR spectroscopy. The presence of carbonate ions in the positions of phosphate ions (carbonate hydroxyapatite of B type) [45] is identified by the absorption bands of bending vibrations ν_3 of O-C bonds ($1420\text{--}1470\text{ cm}^{-1}$) (see Fig. 4, a). The IR spectra of the samples contain weak absorption bands of O-H bond vibrations characteristic of adsorbed crystal water (1630 bending ν_2 , $3400\text{--}3440\text{ cm}^{-1}$ stretching ν_1). The IR spectra of HAP-01 and HAP-02 samples (see Fig. 4, a) contain also a weak band at 3645 cm^{-1} which is due to the stretching vibrations of OH^- group of calcium hydroxide which is formed as a result of wa-

ter vapour sorption from the air by calcium phosphate during mechanochemical synthesis.

In the increased scale, the IR spectra of mechanochemically synthesized Si-HAP samples (see Fig. 4, b) contain weak absorption bands within the range $650\text{--}900\text{ cm}^{-1}$. The authors of [6, 7] relate the bands in this wavenumber range to Si-O bond absorption in AHP structure. The revealed absorption bands with wavenumbers 600 , 675 and 700 cm^{-1} can be attributed to ν_2 of the symmetrical bending vibrations of O-Si-O bonds in HAP structure, while the band at 890 cm^{-1} relates to ν_1 of symmetrical stretching vibrations of Si-O bonds.

Several mechanisms of substitutions during HAP modification with silicate ions were proposed in literature [4, 6, 7, 9]. In the samples

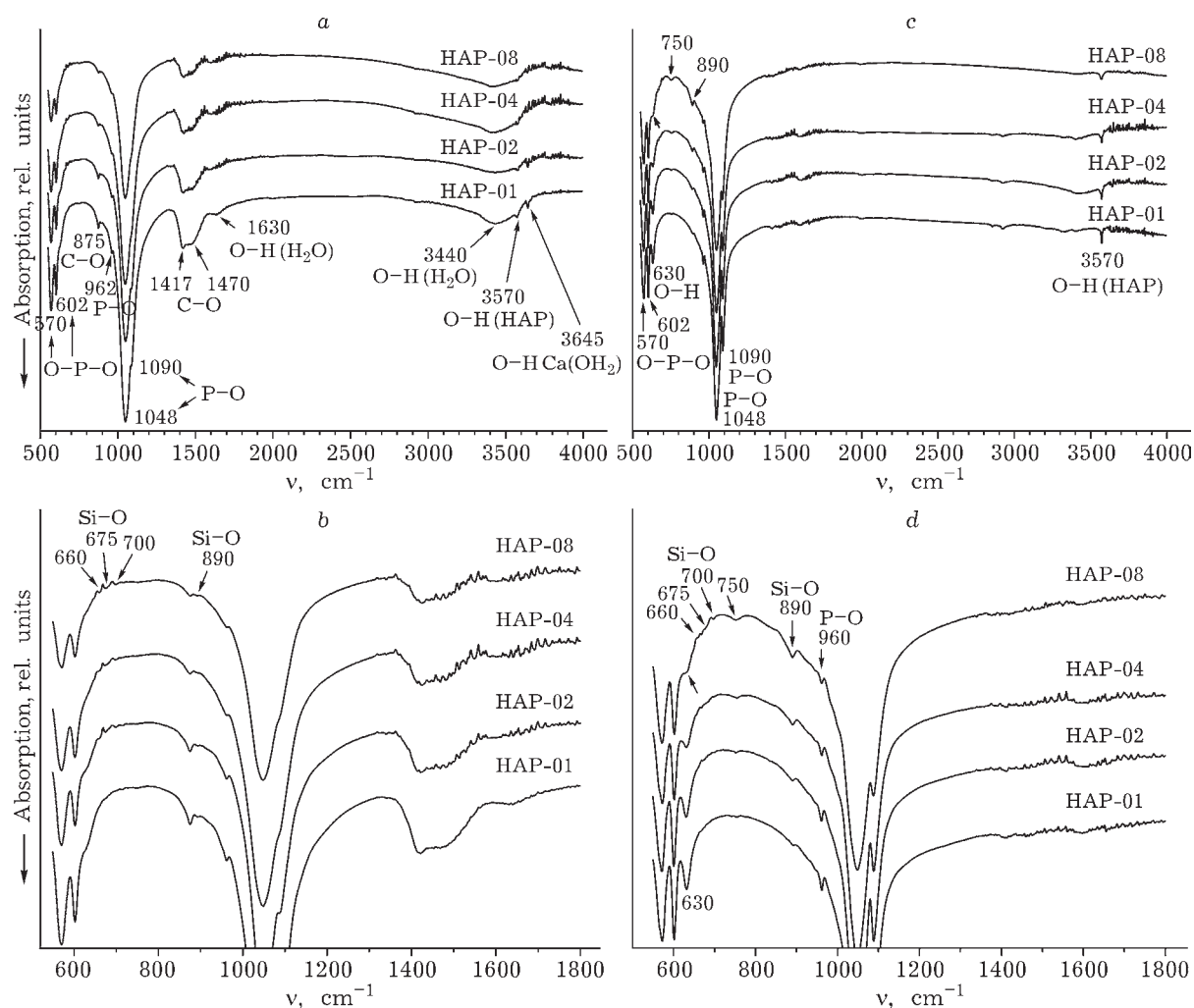


Fig. 4. IR spectra of Si-HAP samples before (a, b) and after (c, d) annealing: a, c - general view; b, d - scaling to $500\text{--}1800\text{ cm}^{-1}$.

of Si-HAP obtained by precipitation [9, 10], carbonate ion in the position of phosphate is always present in HAP structure, that is, carbonate apatite of B type is always formed in the synthesis. A given amount of substituting silicate cannot be completely included into HAP structure during carbonate inclusion. According to the data of the authors of [6], silicone not included into apatite structure is deposited together with HAP as amorphous calcium silicate or silicon hydroxide [7, 9].

The authors of [6] proposed two substitution mechanisms. According to the first mechanism, the formed product can be considered as a solid solution of two other solid solutions – carbonate hydroxyapatite and silicate hydroxyapatite, and the amount of substituted phosphate will be equal to the sum of silicate and carbonate groups with general formula $\text{Ca}_{10-y}(\text{PO}_4)_{6-x}(\text{CO}_3)_y(\text{SiO}_4)_w(\text{OH})_{2-x}$ where $x = w + y$. Thus originating calcium and silicate deficiency can be present as a separate second phase, in particular as amorphous calcium silicate CaSiO_3 . Judging from the carbonate content of the samples synthesized by the authors of [6], this mechanism can be implemented at $y \leq 0.5$. The second mechanism implies the substitution of two phosphate groups for carbonate and silicate ions. The maximal number of substitutions according to this mechanism is possible up to $x = 0.4$ [6].

Other hypotheses if substitutions assume the presence of HPO_4 groups and the deficit of calcium ions, the formation of oxyapatite with partial localization of O^{2-} ions on the 6_3 axis and other versions [9, 10]. According to the data of the majority of published works, silicate is usually localized in the annealed samples in the position of phosphate ion with the formation of a vacancy at the position of OH groups at the 6_3 axis [9, 7, 10]. Analysis of the proposed mechanisms of heteroionic substitution of phosphate by silicate in HAP is presented in [19].

The mechanism of substitutions realized during the mechanochemical synthesis of HAP must differ from that for precipitation from solution. According to the data of [4, 6, 7, 9], with an increase in the concentration of silicate ions in Si-HAP synthesized from solutions the concentration of carbonate ion in the structure increases. In our case, quite contrary, with

TABLE 2

Concentrations of CO_3^{2-} and CO_3 in Si-HAP samples

Samples	CO_2 , mass %	CO_3^{2-} , mass %	CO_3^{2-} , mol
HAP-01	2.8	3.82	0.64
HAP-02	2.6	3.57	0.59
HAP-04	1.8	2.45	0.4
HAP-08	1.4	1.91	0.32

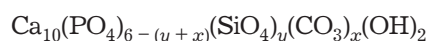
an increase in the amount of silicon introduced the content of carbonate ion decreases. Thus, in HAP-08 sample its content is two times smaller than in HAP-01 sample (Table 2). This is also indicated by a decrease in the intensity of absorption bands of CO_3^{2-} group with an increase in the amount of silicate introduced (see Fig. 4, a, b). For the small amount of silicate introduced, the content of carbonate in HAP structure is higher; after the introduction of silicate in the amount of 0.4 moles both groups are present in equal concentrations, while for 0.8 mol of silicon the amount of carbonate is almost 2.5 times smaller (see Table 2).

For the simultaneous substitution of phosphate for silicate and carbonate ions, competing processes of charge compensation take place. During substitution, the compensation of phosphate charge by carbonate can occur due to the formation of vacancies in calcium position, while for substitution with silicate this may occur due to the vacancies in the position of $(\text{OH})^-$ group. Substitution mechanism may change with the changes in the ratio of carbonate and silicate ions. In the case when the concentration of carbonate ion is higher, the composition of HAP-01 and HAP-02 samples can be represented by the general formula



and the samples will correspond to the following composition: HAP-01 – $\text{Ca}_{9.73}(\text{PO}_4)_{5.26}(\text{SiO}_4)_{0.1}(\text{CO}_3)_{0.64}(\text{OH})_2$; HAP-02 – $\text{Ca}_{9.805}(\text{PO}_4)_{5.21}(\text{SiO}_4)_{0.2}(\text{CO}_3)_{0.59}(\text{OH})_2$.

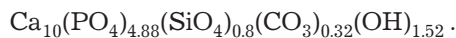
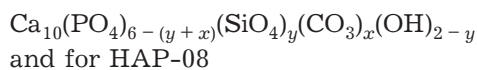
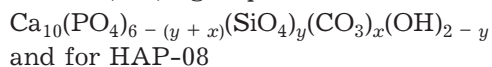
In the case of the equal amount of substituents ($x = y$), the composition of the sample will correspond to the stoichiometric formula without vacancies:



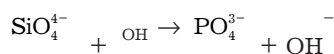
for HAP-04 sample – $\text{Ca}_{10}(\text{PO}_4)_{5.2}(\text{SiO}_4)_{0.4}(\text{CO}_3)_{0.4}(\text{OH})_2$.

If silicate content is higher than carbonate content ($x < y$), charge compensation may occur

due to the formation of vacancies in the position of $(\text{OH})^-$ groups:



After annealing at 1000 °C, substantial changes occurred in the composition of the samples; this affected the absorption bands in IR spectra (see Fig. 4, c, d). In particular, the absorption bands related to carbonate ion and adsorbed water are absent. As the amount of silicate ions in the samples increases, the intensity of absorption bands decreases due to the stretching vibration of bond in O–H group in HAP structure at 3575 cm^{-1} (see Fig. 4, c). With an increase in the concentration of the introduced silicate ion, a decrease in the intensity of absorption bands related to the bending vibrations of O–H bonds at 630 cm^{-1} localized along the *c* axis of HAP structure is observed (see Fig. 4, d). The IR spectra of Si-HAP of the samples with the substitution 0.10.4 moles of silicate (HAP-01–HAP-04) contain the band at 630 cm^{-1} related to the vibration of bonds in OH group, while only a weak shoulder appears in the spectrum of HAP-08 sample (see Fig. 4, d). This is explained by a decrease in the amount of hydroxyl groups localized in channels along the 6_3 axis of HAP structure with the formation of vacancies and charge compensation for the heteroionic substitution of trivalent phosphorus by four-valent silicate according to the scheme



The composition of the synthesized samples after annealing can be represented by the general formula $\text{Ca}_{10}(\text{PO}_4)_{6-x}(\text{SiO}_4)_x(\text{OH})_{2-x}$.

The IR spectra of annealed samples more clearly exhibit absorption bands of Si–O bonds at the wavenumbers of 750 and 890 cm^{-1} , which points to the insertion of silicate ion into HAP structure. These absorption bands, with the intensity increasing as the concentration of inserted silicate increases, are well noticeable on zooming (see Fig. 4, c).

The X-ray diffraction patterns of the samples after mechanical activation of reaction mixtures (see Table 1) in planetary mill for 30 min are shown in Fig. 5. According to the data of X-ray phase analysis, the major part of the sample is HAP phase (sp. gr. *P6₃/m*), small admixtures of CaHPO_4 (sp. gr. *P1*) and $\text{Ca}(\text{OH})_2$ (sp. gr. *P3m1*). The results of the quantitative phase analysis performed using Rietveld method are presented in Table 3. One can see that unreacted monetite CaHPO_4 is present in all the samples. For pure HAP and substituted one with silicon concentration 0.4 and 0.8 mol, monetite concentration does not exceed 2 %; however, in the case of HAP-01 and HAP-02 samples its content is higher. This is likely to be connected with the aggregation of the components of mixtures in these samples, which decreases the rate of interaction. Amorphous silicon oxide prevents aggregation during activation; this may be a reason why the samples with higher silicon concentration contain less admixture of initial substances. The average crystallite size for mechanically synthesized samples with silicon is about 21 nm (see Table 3).

TABLE 3

Results of quantitative analysis and crystallographic characteristics of Si-HAP samples before annealing

Samples	Crystallinity degree, %	Concentration of admixtures, %		HAP crystallite size, nm	HAP unit cell parameters		
		CaHPO_4	$\text{Ca}(\text{OH})_2$		<i>a</i> , Å	<i>c</i> , Å	<i>V</i> , Å ³
HAP-0	82	2	0	19	9.425(2)	6.898(2)	530.7(3)
HAP-0.1	66	8	1	21	9.425(3)	6.905(2)	531.2(3)
HAP-0.2	65	9	3	26	9.422(3)	6.900(2)	530.5(3)
HAP-0.4	57	1	0	18	9.420(3)	6.902(3)	530.5(4)
HAP-0.8	45	<1	0	19	9.421(3)	6.901(3)	530.4(4)

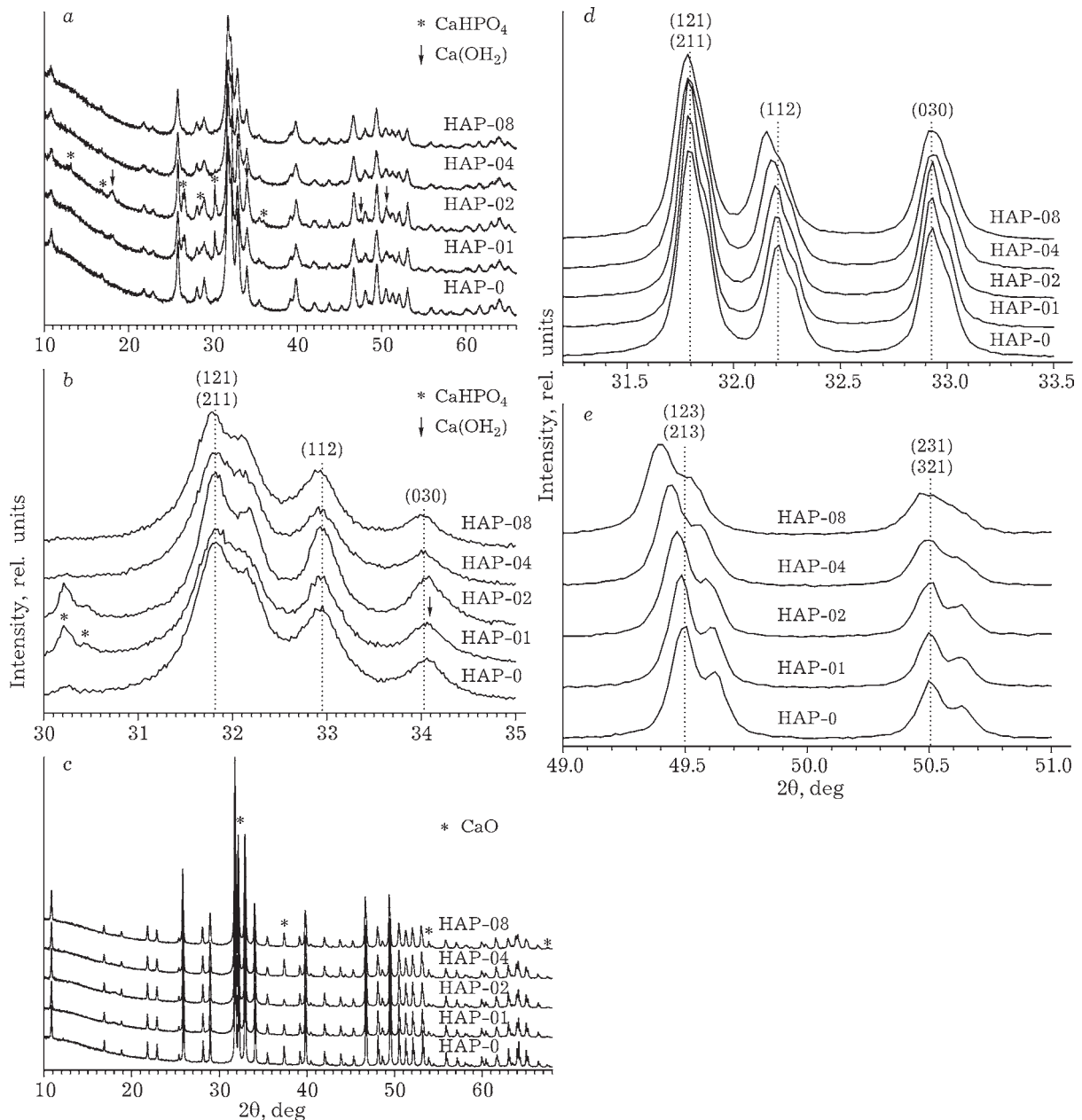


Fig. 5. X-ray diffraction patterns of Si-HAP samples before (a, b) and after (c–e) annealing: a, c – general view; b, d, e – 2θ range, deg: 30–35 (b), 31–32 (d), 49–51 (e).

It was established when refining the cell parameters of mechanochemically synthesized samples of Si-HAP that with an increase in the concentration of introduced silicon, an increase in the amount of the amorphous phase, insignificant changes of *a* and *c* parameters, and cell volume are observed (see Table 3). Because of the low accuracy of cell parameters determination (due to the small particle size), these values can be considered to be almost unchanged. Similar changes in the amount of the

amorphous phase in non-annealed samples were observed also by other authors [7, 9, 10]; however, in these works cell parameters increase with an increase in silicon concentration. This difference can be connected with different synthesis conditions and different initial reagents.

As a result of annealing mechanochemically activated Si-HAP samples, reflections in diffraction patterns became narrow (see Fig. 5, c). One can see that some reflections shifted to smaller angle range, which points to an increase

TABLE 4

Results of quantitative analysis and crystallographic characteristics of Si-HAP samples after annealing

Samples	Crystallinity degree, %	Concentration of CaO admixtures, %	HAP crystallite size, nm	HAP unit cell parameters		
				a , Å	c , Å	V , Å ³
HAP-0T	72	2	180	9.4213(2)	6.8817(2)	528.99(3)
HAP-0.1T	75	1	161	9.4208(3)	6.8847(3)	529.17(3)
HAP-0.2T	74	<1	167	9.4211(3)	6.8878(3)	529.43(3)
HAP-0.4T	75	2	126	9.4229(3)	6.8938(3)	530.09(3)
HAP-0.8T	77	1	111	9.4233(3)	6.9011(3)	530.71(3)

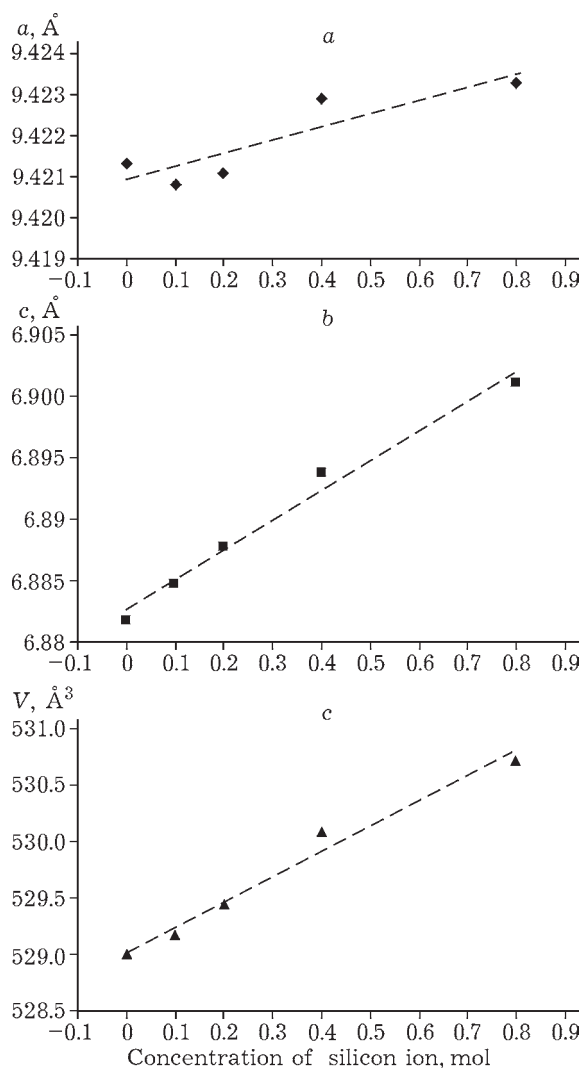


Fig. 6. Change of parameters a (a), c (b) and cell volume (c) of annealed Si-HAP samples depending on the amount of introduced silicon.

in unit cell volume (see Fig. 5, d , e). It was established when refining lattice parameters that parameters a and c are observed to increase (Table 4) with an increase in the concentration of Si atoms in these samples; the maximal growth in exhibited by parameter c . Parameter a is less sensitive to substitution, which agrees with the data reported in [7, 9]. It follows from the data shown in Fig. 6 that the changes of cell parameters and volume are close to the linear dependence. If we take into account the fact that the Si–O interatomic distance is longer than P–O, this is the evidence of the substitution of PO_4^{3-} tetrahedral by SiO_4^{4-} .

Monetite was not detected in samples after annealing (see Table 4). Only CaO in the amount less than 2 % is observed as admixture. It may be assumed that the appearance of CaO in annealed samples, in which this phase was not detected before annealing, is due to partial decomposition of carbonate group during annealing.

Comparative analysis of the data shown in Tables 3 and 4 shows that an increase in crystallinity degree occurs after annealing in all samples containing silicon, that is, the amount of the amorphous component decreases and crystallite size increases substantially. The amount of the amorphous phase in annealed samples is independent of the concentration of silicate ion; crystallite size in them decreases with an increase in the concentration of SiO_4^{4-} .

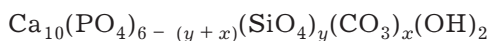
CONCLUSION

The samples of hydroxyapatite modified by silicate ions were synthesized in the crystalline state using the mechanochemical method in a

planetary mill during activation for 30 min. According to the data of HRTEM, the activation of the reaction mixture is accompanied from the very first seconds by the interaction of hydrophosphates with calcium oxide and continues according to the type of neutralization reaction which is characteristic of soft mechanochemical synthesis.

According to the data of EDX and IR spectroscopy, the samples synthesized mechanochemically contain some amount of silicon. During the mechanochemical synthesis of HAP, carbonate ion from atmospheric CO₂ is included into the structure, which results in carbonate apatite of B type. As the concentration of introduced silicon increases, the concentration of carbonate ion decreases. The mechanism of substitution with the changes of the ratio of carbonate and silicate ions in the structure of Si-HAP is likely to change. When the concentration of carbonate ions in Si-HAP structure exceeds the concentration of silicate ion, the composition of Si-HAP can be represented by the general formula

$\text{Ca}_{10-(x-y)/2}(\text{PO}_4)_{6-(y+x)}(\text{SiO}_4)_y(\text{CO}_3)_x(\text{OH})_2$ ($x > y$). In the case of the equal number of substituents ($x = y$), the composition of the sample will correspond to the stoichiometric formula without vacancies:



If the concentration of silicate ions is higher than carbonate ions ($x < y$), charge compensation can occur due to the formation of vacancies in the positions of OH groups:



According to the data of quantitative X-ray phase analysis of non-annealed samples of hydroxyapatite modified by SiO₄⁴⁻ ions, silicon is localized mainly in the amorphous phase because the amount of this phase increases with an increase in the concentration of introduced silicon; the cell parameters of the crystalline phase of HAP do not change.

After annealing, according to the data of IR spectroscopy, carbonate ions and adsorbed water are absent from the samples. As a result of thermal treatment, HAP modified by silicon gets crystallized and undergoes the transformation from the amorphous phase into crystalline one. In this case the amount of the amor-

phous phase does not depend on the concentration of silicon ions introduced into the sample, while the parameters of HAP cell increase linearly with an increase in the concentration of SiO₄⁴⁻. In addition, a decrease in the size of HAP crystallites is observed. The composition of the synthesized samples after annealing can be represented by the general formula $\text{Ca}_{10}(\text{PO}_4)_{6-x}(\text{SiO}_4)_x(\text{OH})_{2-x}$.

The studied products are promising for use as the material to coat implants.

REFERENCES

- 1 Hench L. L., Jones J. R., *Biomaterials, Artificial Organs and Tissue Engineering*, Woodhead Publishing, Cambridge, 2005; Shpak A. P., Karbovskiy V. L., Tarachevskiy V. V., *Apatity, Akadempereodika*, Kyiv, 2002.
- 2 Elliott C., *Structure and Chemistry of Apatite and Other Calcium Orthophosphates*, Elsevier, Amsterdam *etc.*, 1994.
- 3 Porter A. E., Patel N., Skepper J. N., Best S. M., Bonfield W., *Biomaterials*, 25, 16 (2004) 3303.
- 4 Gibson I. R., Best S. M., Bonfield W., *J. Am. Ceram. Soc.*, 85, 11 (2002) 2771.
- 5 Hing K. A., Revell P. A., Smith N., Buckland T., *Biomaterials*, 27, 29 (2006) 5014.
- 6 Palard M., Champion E., Foucaud S., *J. Sol. St. Chem.*, 181 (2008) 1950.
- 7 Arcos D., Rodríguez-Carvajal J., Vallet-Regí M., *Chem. Mater.*, 16, 11 (2004) 2300.
- 8 Leventouri Th., Bunaciu C.E., Perdikatsis V., *Biomaterials*, 24 (2003) 4205.
- 9 Gomes S., Renaudin G., Mesbah A., Jallot E., Bonhomme C., Babonneau F., Nedelec J.-M., *Acta Biomaterialia*, 6, 8 (2010) 3264.
- 10 Mostafa N. Y., Hassan H. M. and Abd Elkader O. H., *J. Am. Ceram. Soc.*, 94, 5 (2011) 1584.
- 11 Guth K., Campion C., Buckland K., Hing A., *Adv. Eng. Mater.*, 12, 1-2 (2010) B26.
- 12 Porter A. E., Buckland T., Hing K., Best S. M., Bonfield W., *J. Biomed. Mater. Res. Part A*, 78A, 1 (2006) 25.
- 13 Patel N., Brooks R. A., Clarke M. T., Lee P. M. T., Rushton N., Gibson I. R., Best S. M., Bonfield W., *J. Mater. Sci.: Mater. in Med.*, 16 (2005) 429.
- 14 Hench L. L., *J. Am. Ceram. Soc.*, 81, 7 (1998) 1705.
- 15 Veresov A. G., Putlyaev V. I., Tretyakov Yu. D., *Ros. Khim. Zh.*, XLVIII, 4 (2004) 52.
- 16 Khlusov I. A., Pichugin V. F., Gostishchev E. A., Sharkeev Yu. P., Surmenev R. A., Surmeneva M. A., Legostaeva E. V., Chaikina M. V., Dvornichenko M. V., Morozova N. S., *Byull. Sib. Med.*, 3 (2011) 72.
- 17 Vandiver J., Dean D., Pate N., Botelho C., Best S., Santos J. D., Lopes M. A., Bonfield W., Ortiz C., *J. Biomed. Res.*, 78A (2006) 352.
- 18 Kanazawa T., *Inorganic Phosphate Materials*, Elsevier, Amsterdam, 1989.
- 19 Gomes S., Nedelec J.-M., Jallot E., Sheptyakov D., Renaudin G., *Crystal Growth & Design*, 11 (2011) 4017.

- 20 Villacampa A. I., Garcia-Ruiz J. M., *J. Crystal Growth*, 211 (2000) 111.
- 21 Nemoto S. R., Nakamura S., Isobe T., Senna M., *J. Sol-Gel Sci. Technol.*, 21 (2001) 7.
- 22 Liao J., Hamada K., Senna M., *J. Mater. Synth. Proc.*, 8, 5 (2000) 305.
- 23 Ting Tian, Dongliang Jiang, Jingxian Zhang, Qingling Lin, *Mater. Sci. Eng.*, c 28 (2008) 57.
- 24 Davidenko N., Carrodegua R., Peniche C., Solis Y., Cameron R., *Acta Biomaterialia*, 6 (2010) 466.
- 25 Paljar K., Orlić S., Tkalčec E., Ivanković H., in: *Matrib 2008 (Proceedings)*, in K. Grilec, G. Marić, S. Jakovljević (Eds.), Hrvatsko društvo za materijale i tribologiju, Zagreb, 2008, pp. 247–254.
- 26 Chaikina M. V., *Mekhanokhimiya Prirodnikh i Sinteticheskikh Apatitov*, Izd-vo SO RAN, Novosibirsk, 2002.
- 27 Chaikina M. V., *Khim. Ust. Razv.*, 6, 2–3 (1998) 141.
- 28 Chaikina M. V., *Fiz. Mezomekhanika*, 7, 5 (2004) 101.
- 29 Chaikina M. V., Khlusov I. A., Karlov A. V., Paichadze K. F., *Chem. Sustain. Dev.*, 12, 3 (2004) 389.
URL: <http://www.sibran.ru/en/journals/KhUR>
- 30 Nakamura S., Isobe T., Senna M., *J. Nanoparticle Res.*, 3 (2001) 57.
- 31 Hui Gang Zhang, Qingshan Zhu, Zhao Hui Xie, *Mater. Res. Bull.*, 40 (2005) 1326.
- 32 Zakharov N. A., Toropov Yu. P., Klyuev V. A., Orlovskiy V. P., *Pis'ma v ZhTF*, 27, 17 (2001) 76.
- 33 Yeong Bernard, Junmin Xue, Wang John, *J. Am. Ceram. Soc.*, 84, 2 (2001) 465.
- 34 Akihiko Yoshida, *J. Biomater. Appl.*, 21, 2 (2006) 179.
- 35 Salaz J., Benzo Z., Gonzalez G., *Rev. Latin. Am. Met. Mat.*, 24, 1–2 (2004) 12.
- 36 Briak-BenAbdeslam H. El., Ginebra M. P., Vert M., Boudeville P., *Acta Biomaterialia*, 4, 2 (2008) 378.
- 37 Никиевич I., Матриж M., Uskoković, Science of Sintering: Current Problems and New Trends. Beograd, 2003, pp. 209–215.
- 38 Shemyakina I. V., Mukhin V. V., Medvedko O. V., Aronov A. M., IV Vseros. Konf. po Nanomaterialam "NANO-2011", Moscow, 2011, p. 170.
- 39 Lurie Yu. Yu., *Spravochnik po Analiticheskoy Khimii, Khimiya*, Moscow, 1965, p. 120.
- 40 EVA, version 14.0, Bruker AXS, Karlsruhe, Germany, 2007. URL: <http://www.bruker-axs.com>.
- 41 Powder Diffraction File – version 2.0804, ICDD, the USA, 2008. URL: <http://www.icdd.com>
- 42 TOPAS, version 4.2, Bruker AXS, Karlsruhe, Germany, 2009. URL: <http://www.bruker-axs.com>
- 43 Inorganic Crystal Structure Database, version 2006-1, FIZ, Karlsruhe, Germany, 2006.
URL: <http://www.fiz-karlsruhe.de/icsd.html>
- 44 Scardi P., Leoni M., *J. Appl. Cryst.*, 39 (2006) 24.
- 45 Le Geros R. Z., Trautz O. R., Le Geros J. P., *Bull. Soc. Chim. France*, 1968. Num. Spec. P. 1712–1717.